J|A|C|S COMMUNICATIONS

Published on Web 05/14/2010

Synthesis and Electrocatalytic Properties of Cubic Mn−Pt Nanocrystals (Nanocubes)

Yijin Kang[†] and Christopher B. Murray*[,†,‡]

Department of Chemistry and Department of Material Science and Engineering, University of Pennsylvania, Philadelphia, Pennsylvania 19104

Received January 26, 2010; E-mail: cbmurray@sas.upenn.edu

Proton-exchange membrane (PEM) fuel cells are receiving increasing attention as high-efficiency energy conversion devices for transportation and mobile applications.[1,2] Platinum (Pt) and Pt-based catalysts are the most popular and effective electrocatalysts for both the anode and the cathode of PEM fuel cells,[1,2] however, slow kinetics at the cathode,[2] high cost,[2] and poor stability remain obstacles to wider adoption.[2,3] Recent efforts to improve the performance of Pt-based catalysts have focused on controlling the composition,[2,4−14] size,[2,15] and shape[16−20] of the materials.

Manganese oxides are widely used as oxygen reduction reaction (ORR) catalysts in alkaline environments, but the acidic environment in PEM fuel cells limits the application of manganese oxides.[2] Alloying Mn and Pt may provide a less expensive, more active catalyst in acidic media. For instance, it has been reported that PtMn/C had better ORR activity than Pt/C.[4] Recent reports have also suggested that the nanocrystal (NC) shape has a dramatic catalytic effect.[16,18,21,22] Markovic et al.[23] reported that the ORR activity of Pt is higher on the (100) faces than on the (111) faces in H_2SO_4. Moreover, a cubic shape exposing (100) surfaces was found to benefit a number of catalytic systems.[16,18] Here we describe the low-temperature solution-phase synthesis of cubic Mn−Pt NCs and studies of their ORR and small-organic-molecule oxidation activities.

The synthesis of Mn−Pt NCs using platinum acetylacetonate [$Pt(acac)_2$] and either manganese acetylacetonate [$Mn(acac)_2$] or dimanganese decacarbonyl [$Mn_2(CO)_{10}$] as precursor has been reported previously.[24,25] To synthesize cubic Mn−Pt NCs, we dissolved $Pt(acac)_2$ in benzyl ether or phenyl ether in the presence of oleic acid and oleylamine and then injected a $Mn_2(CO)_{10}$ stock solution at 160 °C; this was followed by rapid heating of the solution to 200−205 °C, where the solution was kept for 30 min. Transmission electron microscopy (TEM) images of the as-synthesized nanocubes are shown in Figure 1A and Figure S1 in the Supporting Information; images of self-assembled nanocubes are shown in Figure 1B−D. The average edge length of the Mn−Pt nanocubes was 7.7 nm (σ = 6.0%). The combination of oleic acid and oleylamine was essential to obtain particles of uniform size and shape (Figures S5 and S6). The as-synthesized nanocubes were chemically disordered, with Mn and Pt in an fcc unit cell of the *A*1 phase. After the nanocubes were annealed at 600 °C for 30 min, the nanocube structure was converted from the *A*1 phase to the ordered *L*12 phase ($AuCu_3$ structure; Figure 1F). The annealed nanocubes were identified as $MnPt_3$ (JCPDS 65-3260) by powder X-ray diffraction (XRD). Manganese carbide was identified as an impurity in the annealed sample; it was presumably formed from carbonized ligands and traces of excess manganese. The impurity peaks could be removed by UV−ozone treatment (Figure S12). In the XRD patterns, the enhanced (200) peak intensities came from the (100) textured assembly as a result of the preferred orientation

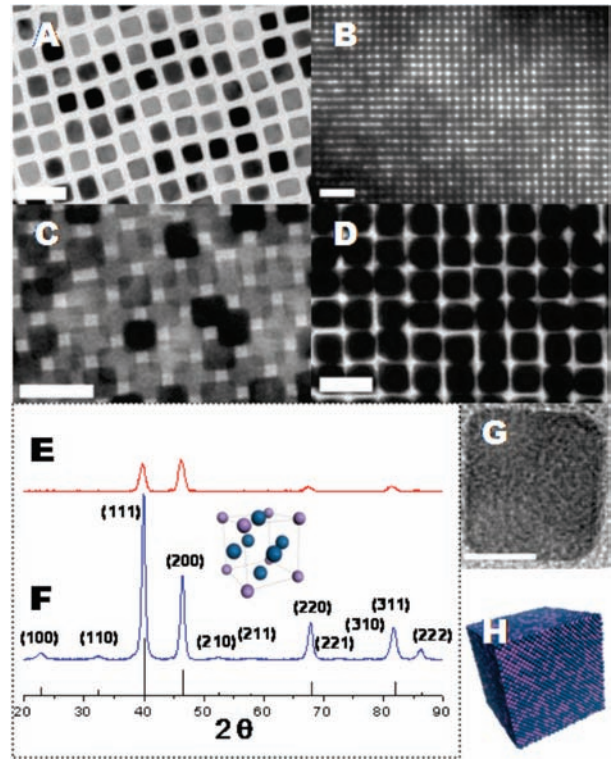

Figure 1. (A−D) TEM images of (A) as-synthesized Mn−Pt nanocubes, (B) a large area of self-assembly, and (C, D) self-assembled Mn−Pt nanocubes. (E, F) XRD patterns of UV−ozone-treated Mn−Pt nanocubes (E) before and (F) after annealing at 600 °C. The inset shows the $MnPt_3$ unit cell. (G) High-resolution TEM image of Mn−Pt nanocubes. (H) Model representing as-synthesized Mn−Pt nanocubes with a disordered structure. Scale bars: 20 nm for (A, C, D); 50 nm for (B); 5 nm for (G). Purple and blue balls represent Mn and Pt atoms, respectively. The annealed sample in (F) confirmed the general stoichiometry of Mn/Pt = 1:3.

of the cubic NCs. The Mn/Pt ratio, which was close to 1:3, was confirmed by both energy-dispersive X-ray (EDX) spectroscopy (Mn/Pt = 22:78; Figure S2) and inductively coupled plasma−optical emission spectrometry (ICP−OES) (Mn/Pt = 27:73). Interestingly, the Mn:Pt ratio remained at 1:3 or less, regardless of whether excess Mn precursor was added. This 1:3 Mn/Pt ratio is consistent with the published result of Lee et al.[25] Spherical Mn−Pt NCs (Figure S4), which are actually polyhedra enclosed by (100) and (111) facets, could also be synthesized by including $Mn_2(CO)_{10}$ as a starting material instead of utilizing hot injection at 160 °C. This synthesis of spherical Mn−Pt NCs is similar to those reported by Lee[25] and Ono.[24]

Figure 2A shows the ORR polarization curves for as-synthesized cubic Mn−Pt NCs, commercial ETEK Pt catalysts, and Pt black. In the kinetically controlled region, the current density on cubic Mn−Pt NCs is higher than those on both the Pt black and ETEK

[†] Department of Chemistry.
[‡] Department of Material Science and Engineering.

10.1021/ja100705j

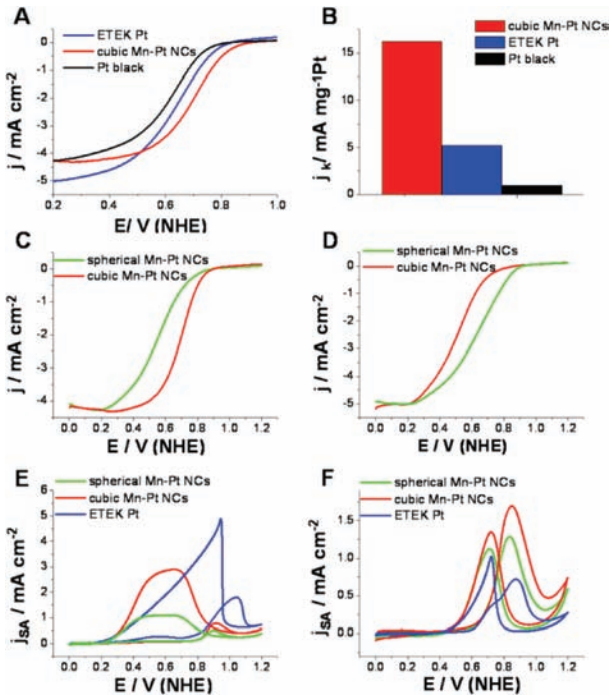

Figure 2. (A) ORR polarization curves for Mn−Pt nanocubes, ETEK Pt, and Pt black normalized to geometric area. (B) Mass activity (as kinetic current densities at 0.8 V) for the three catalysts. (C, D) ORR polarization curves for cubic and spherical Mn−Pt nanocrystals in (C) 0.1 M H_2SO_4 and (D) 0.1 M $HClO_4$. (E) Formic acid and (F) methanol oxidation polarization curves for cubic Mn−Pt nanocrystals, spherical Mn−Pt nanocrystals, and ETEK Pt.

Pt catalysts. Figure 2B shows the kinetic current densities (at 0.8 V) normalized to the effective mass of Pt, which indicate that cubic Mn−Pt NCs are much more active for ORR than the Pt black and ETEK Pt catalysts. The Pt-mass-normalized activity of cubic Mn−Pt NCs is over 3 times greater than that of the commercial catalyst. The ORR activity of Mn−Pt is also shape-dependent (structure-sensitive). The ORR activities of cubic and spherical Mn−Pt NCs in H_2SO_4 and $HClO_4$ are shown in Figure 2C,D, respectively. Interestingly, cubic Mn−Pt NCs show higher ORR activity than spherical Mn−Pt NCs in H_2SO_4, while the spherical NCs are more active in $HClO_4$. This implies that the ORR activity of Mn−Pt NCs is higher on (111) than on (100) in $HClO_4$, whereas the ORR activity is higher on (100) than on (111) in H_2SO_4 because of sulfate anion adsorption.[23] This shape-dependent property of Mn−Pt is very similar to that reported for Pt.[23]

Electrocatalytic properties of cubic and spherical Mn−Pt NCs for formic acid and methanol oxidation were also tested. The polarization curves representing the oxidation activities were normalized to surface areas, which were calculated by measuring the charge of hydrogen adsorption−desorption. To demonstrate that this method is reliable, we used one solution of cubic Mn−Pt NCs to prepare two electrodes with different loadings. The CV curves clearly showed the difference in loading (Figure S10A). After normalization, the formic acid polarization curves for the two electrodes were nearly identical, indicating the constant catalytic activities per unit surface area (Figure S10B). The activities of cubic and spherical Mn−Pt NCs for formic acid and methanol oxidation were compared to those for the ETEK Pt catalyst. For formic acid oxidation, both cubic and spherical Mn−Pt NCs are less active than ETEK Pt, with the cubic Mn−Pt NCs having higher activity than the spherical NCs. However, for methanol oxidation, the cubic Mn−Pt NCs show better activity than ETEK Pt, while spherical Mn−Pt NCs are comparable in activity to ETEK Pt for methanol oxidation. These results suggest that the (100) surface of Mn−Pt is more active for formic acid and methanol oxidation than the (111) surface of Mn−Pt.

In conclusion, we have described the synthesis and characterization of uniform cubic Mn−Pt NCs (nanocubes). The Mn−Pt nanocubes show higher ORR activity than the commercial catalyst. The Mn−Pt nanocubes are also active for small-organic-molecule oxidation and are particularly promising for methanol oxidation. Mn−Pt nanocubes are a potential candidate for both cathode and anode catalysts in fuel cells. In addition, the Mn−Pt NCs show shape-dependent catalytic properties.

Acknowledgment. Y.J.K. and C.B.M. acknowledge the partial financial support from the U.S. Army Research Office (ARO) under Award MURI W911NF-08-1-0364. This research was partially supported by the Nano/Bio Interface Center through the National Science Foundation (NSEC DMR08-32802).

Supporting Information Available: Procedures for synthesis, characterization, and electrochemical measurements; large-area TEM images, XRD patterns, EDX data, and SAED pattern (negative) of Mn−Pt nanocubes; TEM image of spherical Mn−Pt NCs; TEM images in the absence of oleic acid and/or oleylamine; TEM images of nanocubes before and after UV−ozone treatment; TEM images of Pt black and ETEK Pt; and other electrochemistry data. This material is available free of charge via the Internet at http://pubs.acs.org.

References

(1) Steele, B. C. H.; Heinzel, A. *Nature* **2001**, *414*, 345.
(2) Gasteiger, H. A.; Kocha, S. S.; Sompalli, B.; Wagner, F. T. *Appl. Catal., B* **2005**, *56*, 9.
(3) Ferreira, P. J.; la O', G. J.; Shao-Horn, Y.; Morgan, D.; Makharia, R.; Kocha, S.; Gasteiger, H. A. *J. Electrochem. Soc.* **2005**, *152*, A2256.
(4) Mukerjee, S.; Srinivasan, S.; Soriaga, M. P.; McBreen, J. *J. Electrochem. Soc.* **1995**, *142*, 1409.
(5) Stamenkovic, V. R.; Mun, B. S.; Mayrhofer, K. J. J.; Ross, P. N.; Markovic, N. M. *J. Am. Chem. Soc.* **2006**, *128*, 8813.
(6) Stamenkovic, V. R.; Fowler, B.; Mun, B. S.; Wang, G. F.; Ross, P. N.; Lucas, C. A.; Markovic, N. M. *Science* **2007**, *315*, 493.
(7) Stamenkovic, V. R.; Mun, B. S.; Arenz, M.; Mayrhofer, K. J. J.; Lucas, C. A.; Wang, G. F.; Ross, P. N.; Markovic, N. M. *Nat. Mater.* **2007**, *6*, 241.
(8) Zhang, J. L.; Vukmirovic, M. B.; Sasaki, K.; Nilekar, A. U.; Mavrikakis, M.; Adzic, R. R. *J. Am. Chem. Soc.* **2005**, *127*, 12480.
(9) Zhang, J.; Sasaki, K.; Sutter, E.; Adzic, R. R. *Science* **2007**, *315*, 220.
(10) Liu, Q. S.; Yan, Z.; Henderson, N. L.; Bauer, J. C.; Goodman, D. W.; Batteas, J. D.; Schaak, R. E. *J. Am. Chem. Soc.* **2009**, *131*, 5720.
(11) Roychowdhury, C.; Matsumoto, F.; Zeldovich, V. B.; Warren, S. C.; Mutolo, P. F.; Ballesteros, M.; Wiesner, U.; Abruna, H. D.; DiSalvo, F. J. *Chem. Mater.* **2006**, *18*, 3365.
(12) Shevchenko, E. V.; Talapin, D. V.; Rogach, A. L.; Kornowski, A.; Haase, M.; Weller, H. *J. Am. Chem. Soc.* **2002**, *124*, 11480.
(13) Casado-Rivera, E.; Volpe, D. J.; Alden, L.; Lind, C.; Downie, C.; Vazquez-Alvarez, T.; Angelo, A. C. D.; DiSalvo, F. J.; Abruna, H. D. *J. Am. Chem. Soc.* **2004**, *126*, 4043.
(14) Abe, H.; Matsumoto, F.; Alden, L. R.; Warren, S. C.; Abruna, H. D.; DiSalvo, F. *J. Am. Chem. Soc.* **2008**, *130*, 5452.
(15) Aiken, J. D.; Finke, R. G. *J. Mol. Catal. A: Chem.* **1999**, *145*, 1.
(16) Narayanan, R.; El-Sayed, M. A. *Nano Lett.* **2004**, *4*, 1343.
(17) Habas, S. E.; Lee, H.; Radmilovic, V.; Somorjai, G. A.; Yang, P. *Nat. Mater.* **2007**, *6*, 692.
(18) Wang, C.; Daimon, H.; Onodera, T.; Koda, T.; Sun, S. H. *Angew. Chem., Int. Ed.* **2008**, *47*, 3588.
(19) Zhang, J.; Fang, J. Y. *J. Am. Chem. Soc.* **2009**, *131*, 18543.
(20) Housmans, T. H. M.; Wonders, A. H.; Koper, M. T. M. *J. Phys. Chem. B* **2006**, *110*, 10021.
(21) Tian, N.; Zhou, Z. Y.; Sun, S. G.; Ding, Y.; Wang, Z. L. *Science* **2007**, *316*, 732.
(22) Bratlie, K. M.; Lee, H.; Komvopoulos, K.; Yang, P. D.; Somorjai, G. A. *Nano Lett.* **2007**, *7*, 3097.
(23) Markovic, N. M.; Gasteiger, H. A.; Ross, P. N. *J. Phys. Chem.* **1995**, *99*, 3411.
(24) Ono, K.; Okuda, R.; Ishii, Y.; Kamimura, S.; Oshima, M. *J. Phys. Chem. B* **2003**, *107*, 1941.
(25) Lee, D. C.; Ghezelbash, A.; Stowell, C. A.; Korgel, B. A. *J. Phys. Chem. B* **2006**, *110*, 20906.

JA100705J